Polarization infrared spectroscopy study of quasi-orthorhombic acetylene thin films on KCl (100)

Jochen Vogt*
Chemisches Institut der Universität Magdeburg, Universitätsplatz 2, D-39106 Magdeburg, Germany
(Received 28 September 2005; revised manuscript received 10 January 2006; published 22 February 2006)

The growth of ultrathin films of acetylene on KCl (100) single-crystal surfaces has been studied by means of low-energy electron diffraction (LEED) and polarization infrared spectroscopy (PIRS) in transmission geometry at 40 K. IR spectra in the region of the asymmetric stretch vibration ν_3 and the asymmetric bending mode ν_5 were recorded at different coverages. The PIRS spectra as well as the observed $(\sqrt{2}\times\sqrt{2})R45°$ diffraction pattern with two glide planes are consistent with a parallel orientation of the molecules with respect to the surface as expected for the formation of the low-temperature orthorhombic phase of C_2H_2. A refined analysis of the infrared spectra within the dynamic dipole-dipole coupling approach confirms that the lateral orientation of the molecules *within* one layer is close to the T-shaped geometry favored by the intermolecular quadrupole-quadrupole interaction. Deviating from what was assumed in a previous study [J. P. Toennies *et al.*, Phys. Rev. B **65**, 165427 (2002)], the lateral orientation of the molecules in subsequent layers is not characteristic for the orthorhombic phase: essential features in the IR spectra point towards a statistical stacking arrangement of two inequivalent layer types within the films. A structural model is proposed, which is consistent with all available experimental results.

DOI: 10.1103/PhysRevB.73.085418 PACS number(s): 78.67.Pt, 61.14.Hg, 68.65.Ac

I. INTRODUCTION

The study of infrared spectra from acetylene thin films is of interest in the context of the detection of acetylene in interstellar ices[1] and planetary atmospheres.[2] Moreover, infrared spectroscopy is a frequently used tool to investigate the solid-state polymerization of hydrocarbons like acetylene[3,4] and its photochemistry.[5] Assignments to certain structural modifications are often based on the inspection of the shape and position of infrared absorptions.[6] However, a general problem is the detailed understanding how the observed infrared spectra are related to the structure of thin films.[7–9] If the latter are prepared at well-defined surfaces, polarization infrared spectroscopy (PIRS) can provide important information on the orientation of the induced molecular dipole moments and thus on the orientation of molecules. Especially at the surfaces of insulating single crystals, where no induced image dipoles hamper the interpretation of IR spectra recorded with polarized light, this technique shows its strength and essentially improved our knowledge about the structure of molecular adsorbates like CO (Refs. 10–13) or CO_2 (Refs. 14–16).

While the two-dimensional adsorption of acetylene on NaCl(100) has been investigated by means of PIRS,[17] a PIRS study of solid acetylene is missing so far. The reported infrared studies of polycrystalline aggregates of acetylene were based on experiments with unpolarized light, mostly under normal-incidence conditions.[1,2,18–20] For astronomical purposes also the complex refractive index of acetylene films has been tabulated.[2]

The availability of high-quality crystalline films is useful for a clarification of the above-mentioned relation between structure and infrared absorption. Only recently the epitaxial growth of acetylene monolayers and multilayers on KCl (100) single-crystal surfaces was investigated by means of helium atom scattering (HAS).[21,22] A layer-by-layer growth was deduced from oscillations of the specular intensity with increasing exposure and explained by the close match of twice the cation-anion nearest-neighbor distance of KCl with the lattice parameters of orthorhombic acetylene.[22] The first layer forms a $(\sqrt{2}\times\sqrt{2})R45°$ structure with two glide planes, consistent with a parallel orientation of the molecules with respect to the surface plane. It was demonstrated that even the 15th layer maintains this translational symmetry.[22] Based on these results and molecular dynamics (MD) calculations, the structure of acetylene films on KCl (100) was assumed to be close to that of the orthorhombic phase.[22] Orthorhombic acetylene[3,23,24] has a layered structure in which the molecules have a planar orientation with respect to each other. Due to the dominating quadrupole-quadrupole interaction, the neighboring molecules within a layer are arranged in a T-shaped geometry. An angle of 80° is enclosed by their molecular axes.[3] In the case of acetylene thin films on KCl (100), however, the MD calculations[22] predict this angle to be close to 90°.

The goal of this study is a detailed analysis of the PIRS spectra of ultrathin acetylene films on KCl (100), consisting of up to ~6 layers. It is intended to demonstrate that this technique can provide important information on the structure of thin-film molecular crystals in addition to the structure data resulting from diffraction techniques like neutron scattering or helium scattering. Therefore films of various thicknesses were prepared on KCl (100) at a temperature of 40 K and PIRS spectra were recorded in the regions of the two IR-active fundamentals ν_3 and ν_5. In order to establish the experimental relationship to the recent helium diffraction results, low-energy electron diffraction (LEED) measurements accompanied the experiments.

For the modeling of thin-film PIRS spectra the dynamic dipole-dipole coupling approach, as originally introduced by Persson and Ryberg,[25] is used. It is demonstrated that most of the features in the film spectra can be interpreted within this model, which in the past has been successfully applied to

explain monolayer and multilayer spectra of, e.g., CO or CO_2 on various substrates.[12–16] It will be shown that the structure of acetylene ultrathin films is similar to its orthorhombic bulk structure, however with a significant deviation: while the azimuthal orientation of the molecules within one layer is T shaped and the molecular axes are aligned parallel to the KCl (100) substrate surface along the [011] and [01$\bar{1}$] directions, there appears to be no strict correlation of the azimuthal orientation of the molecules in consecutive layers as required for an ideally crystallized film with the orthorhombic bulk structure. Although in conflict with recent MD calculations,[22] these new results are in accordance with the HAS experiments, since thermal energy atom scattering is exclusively sensitive to the topmost surface layer.[26]

This paper is organized as follows: In Sec. II the experimental setup is briefly described and experimental spectra are presented. Section III elucidates the structural models used in this study. Section IV summarizes the methods applied for the simulation of infrared spectra, which are presented in Sec. V. After a detailed discussion of the spectra and the assignment to the proposed structural model the main results are briefly summarized.

II. EXPERIMENT

A. Experimental setup

The experimental setup basically consists of an ultrahigh-vacuum (UHV) chamber which is connected to an evacuable Fourier transform infrared (FTIR) spectrometer (Bruker ifs 120 hr) and an external evacuable detector box. By means of a multi-channel-plate (MCP)LEED optics (Omicron) diffraction experiments with highly insulating crystal surfaces are possible. The experimental setup has already been described in previous publications.[13,27,28] Only the most essential features are therefore presented.

A KCl single crystal (Korth Kristalle) with a front surface area of 20 mm $\times$ 20 mm was cleaved under dry nitrogen atmosphere to give a slice of about 4 mm thickness with two fresh cleavage planes. The latter was mounted on a sample holder and was transferred within 30 min into vacuum. A manipulator allowed the crystal to be rotated and to be adjusted with respect to either the LEED electron gun or the focus of the infrared beam. The latter impinged at the front side of the crystal under oblique incidence conditions ($\beta = 45 \pm 2°$) and left it at its free back side.

The sample holder was connected to the coldhead of a closed cycle helium refrigerator via a copper braid. A minimum temperature of 20 K could be reached, which was measured by means of a silicon diode (LakeShore) at the sample holder near the crystal. Higher temperatures could be set with a stability of 0.1 K by means of an electrically insulated resistance heating. After bakeout a base pressure of 3×10^{-10} mbar was reached. During the experiment the base pressure was below 1×10^{-10} mbar due to the large area of the refrigerator coldhead, which was acting as a cryopump.

Acetylene (purity of 99.6%) was frozen out in a coldfinger, separated from volatile impurities and from its solvent acetone by means of a freezing mixture of pentane and liquid nitrogen. Afterwards the gas was admitted into the UHV chamber by means of a leakage valve. The purity of the adsorptive gas was confirmed by recording mass spectra during the experiment.

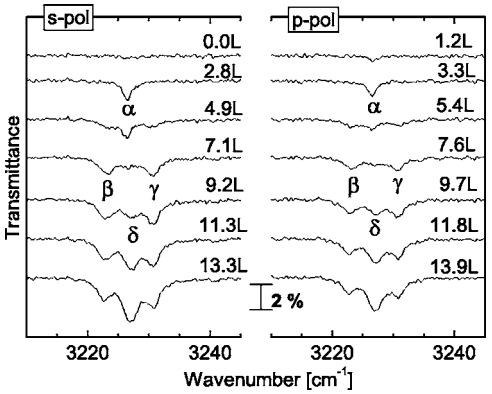

FIG. 1. Experimental PIRS spectra in the region of the ν_3 mode recorded during exposure of a bare KCl crystal to 2.5×10^{-9} mbar acetylene. Each spectrum is labeled with the respective accumulated exposure in units of langmuir (1 L = 10^{-6} Torr s). The sample temperature was 40 K.

Infrared spectra were recorded in transmission geometry at a resolution of 0.2 cm^{-1} by means of a liquid-nitrogen-cooled InSb detector (ν_3 only) or a liquid-nitrogen-cooled MCT detector (ν_3 and ν_5 simultaneously) in the spectral ranges of 2000–4000 cm^{-1} or 600–4000 cm^{-1}, respectively. For the recording of each spectrum 64 interferograms were averaged and Fourier transformed using a Blackman-Harris apodization function. Sample spectra in *s* and *p* polarization were divided by the respective *s*- and *p*-polarized background spectra of the bare crystal.

B. Experimental spectra

In a first experiment the bare KCl (100) crystal was exposed at 40 K to a partial pressure of 2.5×10^{-9} mbar C_2H_2. During exposure infrared spectra were continuously recorded alternately with *s*- and *p*-polarized light. A series of spectra in the region of the ν_3 asymmetric stretch vibration is depicted in Fig. 1. Already after an exposure of 1 L (1 L = 10^{-6} Torr s) a single absorption α appears in *p* polarization at 3227.5 cm^{-1}. After an exposure of 3 L it is also visible in *s* polarization. As discussed below, this infrared band is related to the first acetylene layer on KCl (100). It is the only absorption observed at 75 K, where only the two-dimensional (2D) adsorbate phase is stable at this partial pressure.[29,30] Upon further exposure the monolayer absorption α diminishes while two absorptions β and γ appear at 3223 cm^{-1} and 3231 cm^{-1}, respectively. After 7 L the monolayer peak has almost disappeared in *s* polarization. As further discussed below, the doublet of absorptions β and γ is the spectral signature of a second acetylene layer. After an exposure of 9 L this doublet grows further in intensity, but a further absorption δ near 3227 cm^{-1} develops, which more and more dominates the spectra at higher exposures.

Films of higher quality could be prepared if the first layer was prepared on the KCl (100) surface at 75 K. Then, in a second step, the sample was cooled down to 40 K and was

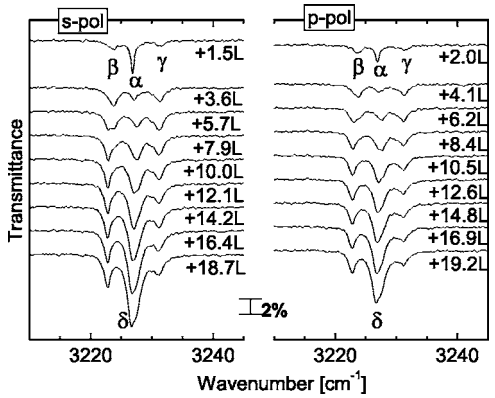

FIG. 2. Experimental PIRS spectra of the ν_3 mode recorded at 40 K during exposure of a monolayer C_2H_2 on KCl (100) to 2.5×10^{-9} mbar acetylene. Each spectrum is labeled with the respective accumulated exposure in addition to the exposure needed to prepare the monolayer at 75 K.

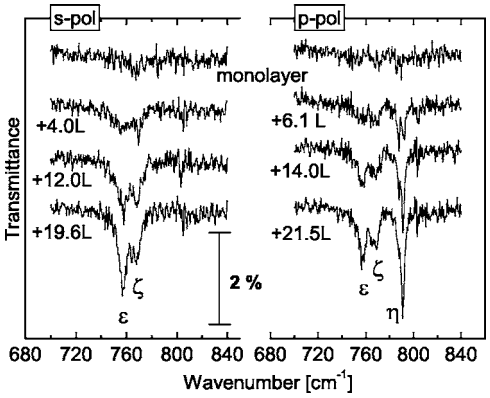

FIG. 4. Experimental PIRS spectra of the ν_5 mode recorded at 40 K during exposure of a monolayer C_2H_2 on KCl (100) to 5×10^{-9} mbar acetylene. Each spectrum is labeled with the respective accumulated exposure in addition to the exposure needed to prepare the monolayer at 75 K.

exposed to acetylene with the same partial pressure as stated above. A series of spectra is shown in Fig. 2. In the first set of spectra the monolayer singlet α is still visible in s and p polarization but the development of the doublet peaks β at 3223.7 cm^{-1} and γ at 3231.3 cm^{-1} indicates the growth of the second layer. With increasing exposure absorption β develops a rapidly growing shoulder at 3222.9 cm^{-1}, while near 3227.5 cm^{-1} the central absorption δ appears. At higher exposures the latter becomes the strongest peak. Apparently it is the superposition of at least two unresolved features.

Three different ν_3 spectra which were recorded in different experiments after exposures of 20 ± 2 L are depicted in Fig. 3 to demonstrate the reproducibility of the film growth. All spectra show the same sequence of absorptions β, γ, δ. The absorptions of film (A) of Fig. 3 are broader than those of films (B) and (C). The latter were grown on a monolayer C_2H_2/KCl (100) at 40 K, which apparently resulted in a higher film quality.

In a third experiment a monolayer of acetylene was again prepared on the bare surface, which was then further exposed

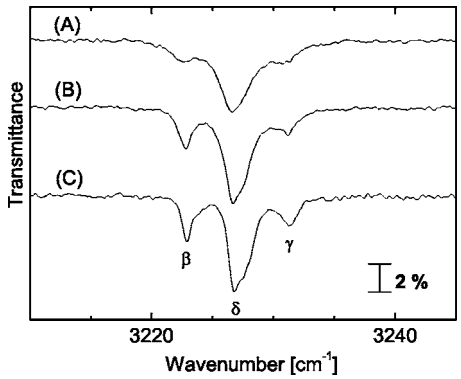

FIG. 3. Comparison between experimental PIRS spectra (p polarization) of the ν_3 mode in different film preparations after an exposure of 20 ± 2 L. (A) Film grown on a bare KCl (100) surface at 40 K. (B) Film grown at 40 K on a monolayer C_2H_2/KCl (100), which was prepared at 70 K. (C) Same as (B) but different KCl (100) single crystal.

to acetylene at a partial pressure of 5×10^{-9} mbar at a crystal temperature of 40 K. Infrared spectra in the region of the ν_5 fundamental, recorded continuously during exposure, are shown in Fig. 4 for s and p polarization, respectively. No absorptions can be unambiguously identified in the topmost pair of spectra, which was recorded at monolayer coverage. After an additional exposure of 4 L a broad feature near 760 cm^{-1} becomes visible in s polarization and also in p polarization, where in addition a split absorption η at 790 cm^{-1} develops. Band η is, however, not visible in s polarization. It is therefore associated with an induced dipole that is oriented perpendicular to the surface plane. At higher dosages only its high-frequency shoulder at 791 cm^{-1} grows further as well as the feature near 760 cm^{-1} seen in s and p polarization. The latter appears to be composed of two IR bands ϵ at 768 cm^{-1} and ζ near 758 cm^{-1}.

In a LEED experiment the acetylene films were prepared in the same way as described above. Diffraction patterns were recorded continuously during exposure. One diffraction pattern (electron energy 140 eV), recorded after an additional exposure of 4.6 L (coverage between 2 and 3 layers), is depicted in Fig. 5. Consistent with the HAS experiments,[22] it reflects a $(\sqrt{2} \times \sqrt{2})R45°$ symmetry of the thin film. No beams of the orders $\{\frac{1}{2}, \frac{1}{2}\}$ and $\{\frac{3}{2}, \frac{3}{2}\}$ were observed over a wide energy range of primary electron energy. This is consistent with the presence of two glide planes in the surface structure[31] formed by the substrate surface layers and the adsorbate molecules. As already discussed in Ref. 21, in this special case of a $(\sqrt{2} \times \sqrt{2})R45°$ structure the two glide-plane axes require a parallel orientation of (at least) two molecules with respect to the surface plane.

The PIRS technique gives direct information on the tilt angle of induced dipole moments via the ratio of integrated absorptions A_s/A_p in s- and p-polarized spectra, respectively.[14,16] The A_s/A_p ratio in the region of the ν_3 fundamental was determined for a single layer at 75 K as well as for multilayer films at 40 K after the exposure was stopped. In both cases $A_s/A_p = 1.55 \pm 0.10$ was obtained, consistent with a tilt angle of $0 \pm 10°$ with respect to the surface plane. Since the ν_3 vibrational mode of C_2H_2 is a "parallel

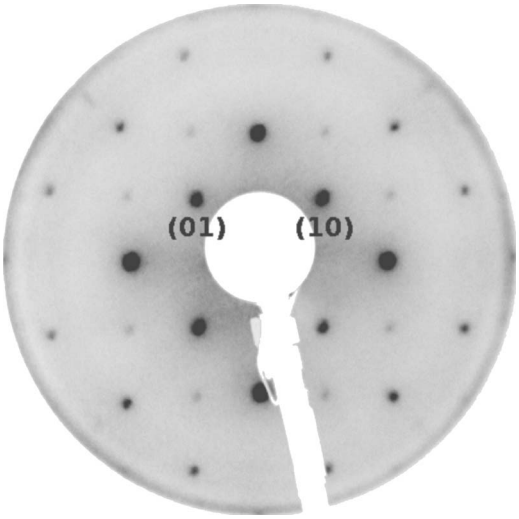

FIG. 5. LEED $(\sqrt{2}\times\sqrt{2})R45°$ diffraction pattern of a multilayer film of acetylene on KCl (100). The primitive reciprocal lattice vectors of the substrate are labeled (10) and (01), respectively. The only visible type of superstructure peaks are $\{\{\frac{3}{2},\frac{1}{2}\}$; the beam orders $\{\frac{1}{2},\frac{1}{2}\}$ and $\{\frac{3}{2},\frac{3}{2}\}$ appear extinguished, consistent with two glide planes along the directions [100] and [010].

mode" with the induced dipole moment oriented along the molecular axis,[32] this tilt angle is identical to the molecular inclination.

III. GROWTH MODELS

Two different structure models for the growth of ultrathin acetylene films were used for the simulation of PIRS spectra presented below. They are based on the experimental results of this study and those of the HAS work[21,22] and consider two inequivalent acetylene molecules in each layer per surface unit cell. These molecules form a planar T-shaped structure. The average angle enclosed by their molecular axes is close to 90°. This can be deduced from the appearance of the singlet absorption α at monolayer coverage. Any angle different from 90° would result in a splitting of the degenerate singlet into a doublet absorption, related to an in-phase and an out-of-phase vibration of the two coupled ν_3 modes within the unit cell.[29,30] A sketch of the monolayer structure is shown in Fig. 6(a) in perspective topview and sideview, respectively. The molecules of the first layer occupy adsorption sites 3.2 Å over the K^+ cations, as favored by a LEED I(V) analysis.[30] Their molecular axes are aligned along the line connecting adjacent cationic sites—i.e., parallel to the [011] and $[01\bar{1}]$ directions, respectively. Deduced from the bulk structure of the orthorhombic phase,[24] the second layer is assumed to occupy adsorption sites over the Cl^- anions, vertically displaced over the first layer by $c=2.79$ Å, which is the layer distance of orthorhombic acetylene.[24] Further layers were assumed to be stacked 2.79 Å above each other and alternately occupy cationic and anionic sites.

A. Model I

The film structures of model I are those of an ideally crystallized film with a structure that is close to that of the orthorhombic phase, as described in the Introduction. Therefore the molecules of the third layer have the same lateral orientation as the equivalent molecules in the first layer, which is illustrated in Fig. 6(b). In a film with an arbitrary number of layers all the molecules above the same site have the same lateral orientation.

B. Model II

The helium atom diffraction experiments[22] provide no evidence that in a multilayer film of acetylene on KCl (100) all molecules above one site have the same orientation. For example, if in the structure given in Fig. 6(b) all molecules in the topmost layer are rotated by 90°, the experimentally observed $(\sqrt{2}\times\sqrt{2})R45°$ symmetry will be maintained. The transformed film structure is sketched in Fig. 6(c). As can be seen there, the molecules over the cationic sites have a crossed planar orientation and, as it turns out, this will affect the coupling of the induced vibrational dipoles within the layer and thus influence the IR spectra. Within model II it is therefore assumed that a layer can have two inequivalent azimuthal orientations, either the regular one called A or the irregular one rotated by 90°, which is called B. Note that the

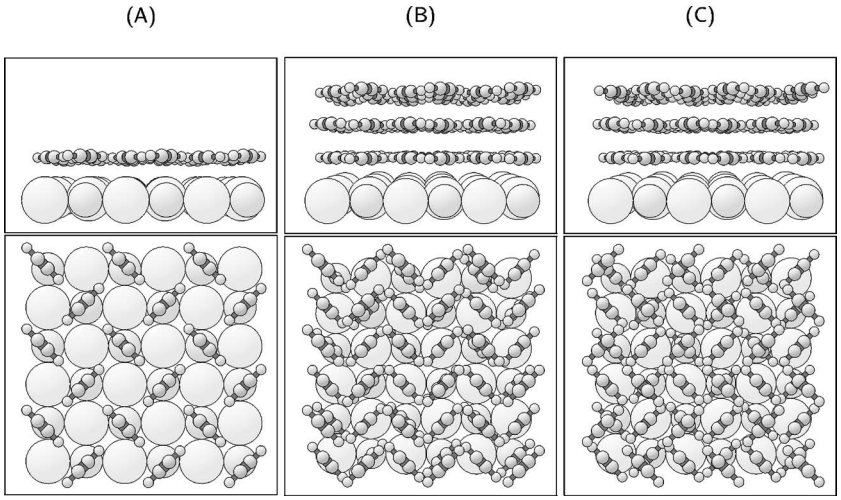

FIG. 6. Structure models of acetylene films on KCl (100) in perspective sideview (top) and topview (bottom). (A) One monolayer with adsorption site over the cations (smaller white balls) exhibiting $(\sqrt{2}\times\sqrt{2})R45°$ symmetry and two glide planes. (B) Three layers with an equivalent orientation of the superimposed molecules in the first and third layers. (C) Three layers with a crossed orientation of the superimposed molecules in the first and third layers. This structure is possible within growth model II (see text), but not within growth model I.

possible bilayer structures AA, AB, BA, and BB can be transformed into each other by rotations of 90°, as well as the monolayer structures. They are thus equivalent due to the C_{4v} symmetry of the KCl (100) surface. *Ad hoc* it is assumed that if a new layer starts to grow, its lateral molecular orientation is of type A or B with equal probability. On a surface which is covered by N layers, this leads to the presence of 2^N different domain structures on the surface. In a refined treatment the assumption of equal probabilities can be modified.

IV. OPTICAL MODEL

If molecules adsorb on a surface, the transition frequencies of their vibrational modes shift with respect to the respective gas-phase values due to the force fields of the substrate and the adjacent molecules. Also the strength of the induced dipole moments is affected, which is specified in this study in terms of the vibrational polarizability[25]

$$\alpha_{\mathrm{vib}} = \frac{2|\boldsymbol{\mu}|^2}{hc\tilde{\nu}_0}, \tag{1}$$

where $\boldsymbol{\mu}$ is the transition dipole moment at the singleton wave number $\tilde{\nu}_0$. If the induced dipole moment of a certain vibrational mode is strong, then its localized character will be lost in the adsorbed state due to a coupling of a molecule's induced dipole moment with the dipole moments in its surrounding. To model this dynamic dipole-dipole coupling, an approach originally used by Persson and Ryberg[25] is applied. This method was successfully used in the past to model IR spectra of adsorbates.[12–14,16] Only the basic relations are therefore shortly summarized in the rest of this section. Consider the external electric field of a plane electromagnetic wave $\boldsymbol{E}(\tilde{\nu})$ at the site of the lth molecule, whose complex polarizability tensor in the spectral region of a certain vibrational mode (Lorentz oscillator with singleton wave number $\tilde{\nu}_0$, width $\Delta\tilde{\nu}$) may be

$$\boldsymbol{\alpha}_l(\tilde{\nu}) = \boldsymbol{\alpha}_e + \frac{\boldsymbol{\alpha}_{\mathrm{vib},l}}{1 - \frac{\tilde{\nu}}{\tilde{\nu}_0}\left(\frac{\tilde{\nu}}{\tilde{\nu}_0} + i\frac{\Delta\tilde{\nu}}{\tilde{\nu}_0}\right)}. \tag{2}$$

The electronic part $\boldsymbol{\alpha}_e$ is assumed to be constant in the considered spectral range. It is well known from classical electrodynamics[33] that the induced electric-dipole moment of the lth molecule in an arbitrary assembly of molecules is

$$\boldsymbol{p}_l = \boldsymbol{\alpha}_l\left(\boldsymbol{E}_l - \sum_{l\neq j}\frac{\boldsymbol{p}_j - 3\boldsymbol{n}_{lj}(\boldsymbol{n}_{lj}\boldsymbol{p}_j)}{r_{lj}^3}\right), \tag{3}$$

where $r_{lj}=|\boldsymbol{x}_l-\boldsymbol{x}_j|$ is the distance between two dipoles located at $\boldsymbol{x}_l$ and $\boldsymbol{x}_j$ and $\boldsymbol{n}_{lj}=(\boldsymbol{x}_l-\boldsymbol{x}_j)/r_{lj}$. For a periodic slab containing S inequivalent molecules this set of equations reduces to $3S$ linear equations for the Cartesian components of S coupled dipole moments,

$$\boldsymbol{p}_s(\tilde{\nu}) = \boldsymbol{\alpha}_s(\tilde{\nu})\left(\boldsymbol{E}_s(\tilde{\nu}) - \sum_{s'}^{S}\boldsymbol{U}_{ss'}\boldsymbol{p}_{s'}(\tilde{\nu})\right), \tag{4}$$

where $\boldsymbol{U}_{ss'}$ is a dipole-sum matrix, in which contributions from neighboring unit cells are summed up. Since the wavelength of infrared radiation is much larger than the considered unit-cell extensions, retardation effects and a dependence on the wave vector of the external field can be neglected.[25] For a given structure model Eq. (4) was solved using standard linear algebra methods. Using Fresnel's laws,[38] different external electric fields for either s and p polarization at the front and back sides of the substrate are taken into account, as explained in Ref. 16. Finally the total absorption $A(\tilde{\nu})$ of the whole layer is calculated via the sum of all molecular absorption cross sections $\sigma_s(\tilde{\nu})$, which are defined as the energy absorbed per unit frequency interval divided by the incident energy flux per unit area per unit frequency,[33] leading to

$$\sigma_s(\tilde{\nu}) = \frac{8\pi^2\tilde{\nu}}{|E|^2}\,\mathrm{Im}[\boldsymbol{p}_s\boldsymbol{E}_s^*], \tag{5}$$

$$T(\tilde{\nu}) \sim 1 - A(\tilde{\nu}) = 1 - \frac{1}{F\cos\beta}\sum_{s}^{S}\sigma_s(\tilde{\nu}), \tag{6}$$

where $T(\tilde{\nu})$ is the transmittance of the film and F the area of the unit cell. Equation (6) is the basis for the simulated transmission spectra presented below. Due to the C_{4v} symmetry of the KCl (100) surface, the adsorbate is expected to be present on the surface in four inequivalent azimuthal domain orientations rotated by 0°, 90°, 180°, and 270° with respect to the crystal [001] direction. The contributions from each of these domains are thus averaged.

V. SIMULATION OF IR SPECTRA

A. Parameter sets

Vibrational polarizabilities and singleton wave numbers were considered as free parameters and were adjusted to give a good reproduction of the positions of the IR absorptions at monolayer and bilayer coverage, while values for the electronic part of the polarizability tensor were taken from Keir *et al.*[34] In the case of the ν_5 mode the parameter sets were optimized to reproduce the band positions of the three visible IR absorptions of the films. A peculiarity of the ν_5-asymmetric bending mode is its twofold degeneracy in the gas phase.[32] Adsorbed on the KCl (100) surface this degeneracy should actually be lifted since the bending mode $\nu_{5\perp}$ perpendicular to the surface and the mode $\nu_{5\|}$ parallel to the surface will belong to different symmetry species of the molecule's site group. Separate sets with slightly different values of the vibrational polarizability and the singleton frequency could be assigned to each of the inequivalent asymmetric bending modes. As seen below, the use of only one set of parameters for both modes is capable of explaining all absorptions seen in the experimental ν_5 spectra.

The chosen sets of parameters are given in Table I together with the resulting absorption cross sections σ_{rand}. The latter are corrected to reflect the cross section of randomly oriented molecules in order to make them comparable to the respective gas-phase values reported in the literature[35,36] (ν_3, 1.2×10^{-17} cm; ν_5, 2.94×10^{-17} cm; see also the discussion in Ref. 17). For the ν_3 mode, Khanna *et al.*[2] report an in-

TABLE I. Sets of singleton wave numbers $\tilde{\nu}_0$ and vibrational polarizabilities α_{vib} used for the simulation of PIRS spectra for the ν_3 and ν_5 fundamental modes. Also given is the resulting absorption cross sections σ_{rand} corrected for random orientation.

Mode		$\tilde{\nu}_0$ [cm^{-1}]	α_{vib} [Å^3]	σ_{rand} [cm]
ν_3	First layer	3229.2	0.125	5.4×10^{-17}
	Second layer	3233.0	0.075	3.2×10^{-17}
$\nu_{5\parallel}$, $\nu_{5,\perp}$		768.0	0.620	1.5×10^{-17}

crease of the absorption cross section by a factor of 3 upon solidification and a decrease of 35% for the ν_5 mode, respectively. This is in reasonable agreement with σ_{rand} calculated from the multilayer parameter set. The cross section of the ν_3 mode for the first layer exceeds the gas-phase value even by a factor of 4.5. This is consistent with the unexpectedly high total integrated absorption of the singlet (peak α) of a saturated monolayer at 75 K, which was determined to be (0.10 ± 0.01) cm^{-1}. Taking into account the 5.07×10^{14} cm^{-2} adsorption sites on an ideal KCl (100) surface, the monolayer cross section in Table I predicts a value of 0.12 cm^{-1} for the total absorption,[39] which is in fair agreement with the experimental value. The elevated absorption cross section is likely due to the substrate force field which leads to a higher vibrational polarizability and, accordingly, to an additional redshift of almost 4 cm^{-1} compared to the singleton frequency of the molecules in the second layer.

The half widths $\Delta\tilde{\nu}_0$ used in the simulations were 1.5 cm^{-1} in the case of the ν_3 fundamental and 4.0 cm^{-1} for the ν_5 mode, respectively. These values were chosen in order to reproduce experimentally observed peak widths.

B. ν_3 mode

With the structure depicted in Fig. 6(a) and the parameter set for the first layer in Table I the above-described dynamic dipole-dipole coupling approach reproduces PIRS spectra with a single absorption at the position where peak α was observed in the experimental spectra. Sets of simulated PIRS spectra are given in Fig. 7, which are identical for model I (diagram A) and model II (diagram B). The stronger absorption in s polarization is consistent with an A_s/A_p ratio of 1.55 and reflects the parallel orientation of the coupled dipole moments with respect to the surface.

If a second layer is added, the resulting ν_3 spectra show a low-frequency absorption at the position of the experimentally observed peak β and a high-frequency band whose position coincides with that of peak γ. For reasons given above in Sec. III the corresponding simulated spectra depicted in Fig. 7 are identical for models I and II.

ν_3 spectra from films of three to six layers are also presented in Fig. 7 (diagram A, model I; diagram B, model II). In the case of model I the spectra show two main absorptions near 3223 and 3232 cm^{-1}, respectively. Between these two major peaks several weak absorptions occur depending on layer thickness. At a coverage of six layers and in thicker films (not shown) these absorptions shift to lower frequencies below 3225 cm^{-1}. While it would be reasonable to identify the two main absorptions at 3223 and 3232 cm^{-1} with the experimentally observed peaks β and γ, band δ is not reproduced with model I. This will be further discussed below in Sec. VI.

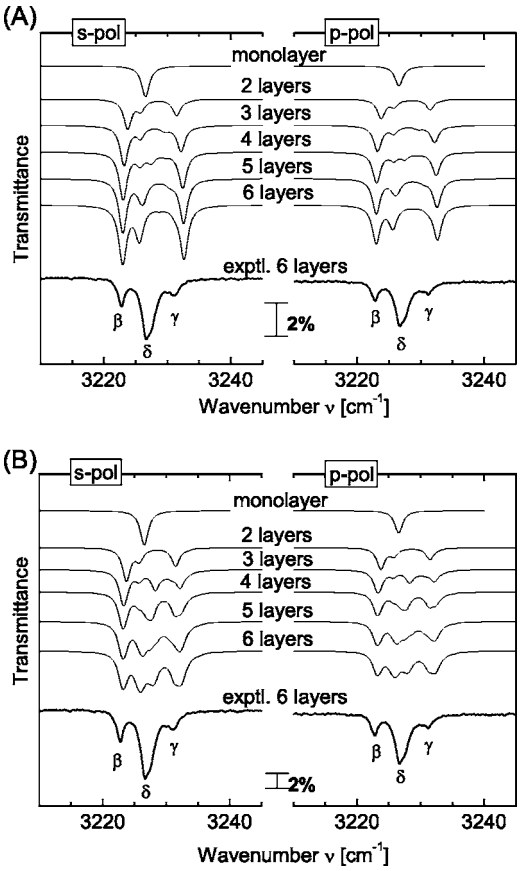

FIG. 7. Calculated PIRS transmission spectra of acetylene multilayers in the region of the ν_3 mode using the parameter set given in Table I. (A) Growth model I and (B) growth model II. As explained in the text, the spectra of model II are the average of spectra from 2^N different film structures of N layers assumed to coexist on the surface with equal abundance. In addition, an experimental PIRS spectrum (bold solid line) of a film containing ~6 layers is shown in each diagram.

In the case of model II the spectra of all possible inequivalent film structures were averaged with equal weights as explained above. Between two low- and high-frequency absorptions near 3223 cm^{-1} and 3232 cm^{-1} a central absorption appears between 3228 and 3226 cm^{-1}, whose shape varies with layer thickness. In a film containing six layers the central absorption develops a shoulder very similar to what was observed for absorption δ in the experimental spectra shown in Fig. 2. While the agreement between the spectra of model II and those of the experiments is thus very good concerning the appearance and position of IR peaks, there are discrepancies in the relative intensities of simulated and observed spectra of films with thicknesses exceeding four layers. Within growth model II this might point towards film structures, which are statistically more abundant on the KCl (100) surface than others. Therefore the spectral contributions of the different film structures were analyzed in detail. For a film containing six layers, the IR spectra of two se-

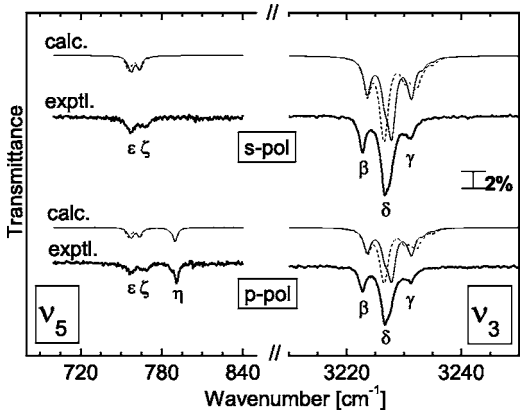

FIG. 8. Comparison between experimental (bold solid line) and calculated PIRS transmission spectra of two selected structural configurations AAABAA (dashed line) and BAABAA (solid line) of an acetylene film containing six layers.

lected configurations are presented in Fig. 8 for the ν_3 as well as for the ν_5 mode. The spectra for the structure AAABAA is shown as a dashed line, while those of structure BAABAA are indicated as a solid line. As further discussed in the next section, the agreement between experimental ν_3 spectra and a superposition of the spectra profiles belonging to these film structures is particularly good.

C. ν_5 mode

The modeling of acetylene film spectra in the region of the ν_5 fundamental was done in the same way as for the ν_3 spectra. PIRS spectra of film structures according to growth model I with thicknesses ranging from one monolayer to six layers are shown in diagram (A) of Fig. 9. At monolayer coverage a doublet of two absorptions is predicted. It consists of a peak near 765 cm^{-1} visible in *s*- and *p*-polarized spectra and a high-frequency peak near 785 cm^{-1}. The latter is only visible in *p* polarization. At higher coverages the low-frequency absorption splits into two peaks, one near 765 cm^{-1} and a second one which shifts from 758 cm^{-1} to 753 cm^{-1} as the number of layers increases. Conversely, the high-frequency absorption is blueshifted with increasing layer thickness towards 791 cm^{-1}. This could explain the initial splitting of band η in the experimental spectra (Fig. 4) during the film growth if a temporal coexistence of film areas with different numbers of layers is assumed.

Averaged PIRS spectra of film structures according to growth model II are shown in diagram (B) of Fig. 4. As has been done in the case of the ν_3 mode, equal probabilities of all possible structural configurations were initially assumed. The spectra of the monolayer and second layer are identical to those of model I since the corresponding structures are equivalent due to symmetry (see Sec. III). The high-frequency absorption, visible only in *p* polarization, shifts towards 791 cm^{-1}, in the same way as calculated with model I. Two absorptions are furthermore visible in the *s* and *p* polarization between 756 cm^{-1} and 764 cm^{-1}. It is reasonable to assign them to the experimentally observed absorptions ϵ and ζ (Fig. 4).

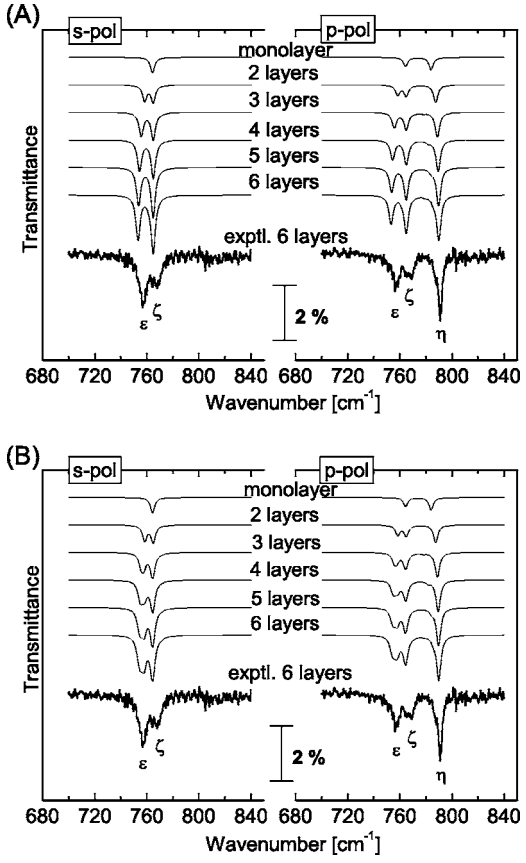

FIG. 9. Calculated PIRS transmission spectra of acetylene multilayers in the region of the ν_5 mode using the parameter set given in Table I. (A) Growth model I and (B) growth model II. As explained in the text, the spectra of model II are the average of spectra from 2^N different film structures of *N* layers assumed to coexist on the surface with equal abundance. In addition, an experimental PIRS spectrum (bold solid line) of a film containing ~6 layers is shown in each diagram.

In Fig. 8 the ν_5 spectra of the two configurations AAABAA and BAABAA of a film containing six layers are plotted separately. Although the agreement with the experimental spectra in Fig. 4 is generally good, the influence of various layer arrangements on the ν_5 spectra is not as pronounced as in the case of the ν_3 fundamental. The nature of the three absorptions ϵ, ζ, and η will be further discussed in the next section.

VI. DISCUSSION

The comparison of the experimental PIRS spectra from acetylene films presented in Sec. II with simulated spectra in Sec. V strongly suggests that the effects of dipole-dipole coupling are responsible for the observed fine structure in the spectra. The sequence (cf. Fig. 1) of a ν_3 singlet, doublet, and triplet absorption during the film growth can be understood within the applied optical model as the spectral signatures of monolayer, bilayer, and multilayer films. The observation of this sequence is thus consistent with the previously reported[22] layer-by-layer growth of acetylene on the KCl

(100) substrate at 40 K. LEED patterns recorded during the film growth reproduce the $(\sqrt{2}\times\sqrt{2})R45°$ symmetry found with HAS for multilayer films. Therefore a direct comparison of the two experiments is justified. Moreover, from the spectra in Figs. 1 and 2 a required exposure of 3–4 L for the growth of a new layer can be determined, consistent with a sticking probability of 0.3–0.4. This is in good agreement with a sticking probability of 0.4 found in the HAS experiments. However, the appearance of the monolayer peak α in Fig. 1 does not support an assumption proposed in the HAS study, according to which the first two layers could grow all at once.[22]

The model of an ideally crystallized film with the bulk structure of the orthorhombic phase (model I) fails to reproduce the observed spectra of multilayer films. In the region of the ν_3 fundamental the appearance of the central absorption δ dominating the spectra at coverages above four layer thickness cannot be modeled [compare Figs. 1 and 2 with Fig. 7(a)] or would at least require the use of very complicated parameter sets, which are not justified by other reasons. The use of significantly different sets of α_{vib} and $\tilde{\nu}_0$ for the molecules in the second, third, and higher layers does not lead to improvements, since this would shift the positions of the high- and low-frequency absorptions dependent on layer thickness. Experimentally, however, only small shifts of peaks β and γ are observed. A reasonable effort to improve the agreement between experimental and simulated spectra could imply changes of the structure parameters of model I: the distance between layers and the azimuthal orientation of the molecules. Moderate variations of these parameters slightly change the peak positions in the spectra of Fig. 7(a) and also affect the relative peak intensities. However, no dramatic improvements could be achieved with these attempts.

Using the simple parameter set given in Table I, an enhanced agreement between simulated and observed ν_3 spectra is obtained if the possibility is taken into account that acetylene layers can grow misoriented by 90° above each other (model II). Having the same $(\sqrt{2}\times\sqrt{2})R45°$ translational symmetry, such structures differ from the orthorhombic bulk geometry, since they allow the linear molecules over one adsorption site to have a crossed lateral orientation with respect to each other. The misoriented growth of a layer is a statistical event. It is thus reasonable to assume that a variety of film structures containing misoriented molecules in different layers will coexist on the surface in a large number of different domains. The experimental infrared spectrum is thus a superposition of spectra from each of these domains and is reproduced in repeated film preparations (see Fig. 3). Accordingly, the modeling of PIRS spectra involved an averaging of contributions from all possible structural configurations which were assumed to coexist on the surface with equal abundance. As can be seen in Fig. 7(b) this growth model reproduces the occurrence of the central absorption δ seen in the experimental multilayer spectra. However, simulated PIRS spectra (Fig. 8) of an acetylene film with six layers and the configurations AAABAA and BAABAA give the best match with the experimental spectra profiles at this coverage. Such structures contain one and two misoriented layers, respectively. MD calculations of acetylene films on KCl (100) (Ref. 22) gave no hints for the existence of such stacking errors. However, the starting geometry of the MD simulations in the cited work was that of an ideally crystallized film. Further theoretical investigations could confirm that films containing misoriented acetylene layers are stable or energetically even slightly more favorable. Since a stacking error of the type described above has no consequences on the structural arrangements of the nearest neighbors, the intralayer "*T* pairings,"[37] the total energy of these film structures should be only slightly different from that of an ideally crystallized film.

Besides the consideration of stacking errors, a more refined analysis should investigate the possible influence of other film imperfections on the spectra, especially the misorientations of molecules within one layer and the effect of finite domain sizes.

The spectra of the ν_5 mode are not as sensitive to details of the film structure as those of the ν_3 mode. Nevertheless, the experimental and simulated PIRS spectra in this spectral range are in good agreement for multilayer films. The high-frequency absorption η is only visible in *p* polarization and has to be assigned to an induced dipole moment perpendicular to the surface. It cannot be excited at normal-incidence conditions and was thus not detected in other thin film studies.[2,18] An analysis of the calculated induced dipole moments of the molecules at the peak frequencies of ϵ, ζ, and η confirms that the two low-frequency absorptions ϵ and ζ visible in *s*- and *p*-polarized film spectra are due to dynamic dipole-dipole couplings of the $\nu_{5\|}$ modes of molecules in different layers. The high-frequency absorption, which is exclusively seen in *p*-polarized spectra, is due to the excitation of the $\nu_{5\perp}$ modes of the molecules. Hence, although the present results do not support significant differences in the transition frequencies of these modes for the single molecule (no site symmetry splitting; see Table I), their collective excitation leads to a marked splitting of about 20 cm^{-1} by means of dipole coupling.

VII. SUMMARY

Polarization infrared spectroscopy is a useful technique for the investigation of ultrathin molecular films, especially in combination with low-energy electron diffraction or helium atom scattering. This has been demonstrated for acetylene monolayer and multilayer films grown on KCl (100) single-crystal surfaces at 40 K.

Recorded in transmission geometry under oblique incidence conditions, PIRS spectra in the region of the ν_3-asymmetric stretch mode show the sequence of a singlet, doublet, and triplet absorption upon exposure of the bare surface, consistent with a previously reported layer-by-layer growth[22] of acetylene on KCl (100). From the ratio of the integrated absorption in *s* and *p* polarization a parallel orientation of the molecules with respect to the surface can be deduced. This agrees well with the presence of two glide planes in the $(\sqrt{2}\times\sqrt{2})R45°$ diffraction pattern observed with LEED and helium scattering.[21,22]

Three absorptions can be distinguished in the region of the ν_5-asymmetric bending mode. The IR band with the highest frequency at 791 cm^{-1} is only visible in *p* polariza-

tion, consistent with an induced dipole moment perpendicular to the surface plane.

On the basis of the dynamic dipole-dipole coupling approach[25] the observed spectra were related to the microscopic structure of the thin films. Derived from the bulk structure of orthorhombic acetylene,[22–24,37] a structure model with a planar T-shaped arrangement of the molecules within the layers led to a good agreement between experimental and simulated spectra for monolayer and bilayer films, respectively. The strongest absorption observed in films of four to six layer thickness, however, cannot be explained with the model of an ideally crystallized film of orthorhombic acetylene. If the presence of azimuthally misoriented layers in the films is taken into account, all observed absorptions in the regions of the ν_3 and ν_5 fundametal modes can be satisfactorily modeled.

ACKNOWLEDGMENTS

I wish to thank Professor H. Weiss for his support of the experimental work of this study, which was in part financed by the Deutsche Forschungsgemeinschaft (DFG). Discussions with Dr. M. Hustedt and Dr. F. Traeger are gratefully acknowledged.

*Electronic address: Jochen.Vogt@VST.uni-magdeburg.DE

[1] N. Boudin, W. A. Schutte, and J. M. Greenberg, Astron. Astrophys. **331**, 749 (1998).
[2] R. K. Khanna, M. J. Ospina, and G. Zhao, Icarus **73**, 527 (1988).
[3] M. Bernasconi, G. L. Chiarotti, P. Focher, M. Parrinello, and E. Tosatti, Phys. Rev. Lett. **78**, 2008 (1997).
[4] M. Ceppatelli, M. Santoro, R. Bini, and V. Schettino, J. Chem. Phys. **113**, 5991 (2000).
[5] S. K. Dunn and G. E. Ewing, J. Vac. Sci. Technol. A **11**, 2078 (1993).
[6] S. Hirabayashi, N. Yazawa, and Y. Hirahara, J. Phys. Chem. A **107**, 4829 (2003).
[7] Y. J. Chabal, Surf. Sci. Rep. **8**, 211 (1988).
[8] V. P. Tolstoy, I. V. Chernyshova, and V. A. Skryshevsky, *Handbook of Infrared Spectroscopy of Ultrathin Films* (Wiley, New York, 2003).
[9] G. A. Baratta, M. E. Palumbo, and G. Strazulla, Astron. Astrophys. **357**, 1045 (2000).
[10] J. Heidberg, M. Suhren, and H. Weiss, J. Electron Spectrosc. Relat. Phenom. **64/65**, 227 (1993).
[11] J. Heidberg, E. Kampshoff, and M. Suhren, J. Chem. Phys. **95**, 9408 (1991).
[12] D. A. Boyd, F. M. Hess, and G. B. Hess, Surf. Sci. **519**, 125 (2002).
[13] J. Vogt and H. Weiss, Z. Phys. Chem. (Munich) **218**, 973 (2004).
[14] J. Heidberg, E. Kampshoff, O. Schönekäs, H. Stein, and H. Weiss, Ber. Bunsenges. Phys. Chem. **94**, 112 (1990).
[15] O. Berg, R. Disselkamp, and G. E. Ewing, Surf. Sci. **277**, 8 (1992).
[16] J. Heidberg, M. Hustedt, E. Kampfshoff, and V. M. Rozenbaum, Surf. Sci. **427–428**, 431 (1999).
[17] S. K. Dunn and G. E. Ewing, J. Phys. Chem. **96**, 5284 (1992).
[18] G. L. Bottger and D. F. Eggers, J. Chem. Phys. **40**, 2010 (1964).
[19] W. M. Hayden Smith, Chem. Phys. Lett. **3**, 464 (1969).
[20] H. Schubert, Ph.D thesis, University of Hannover, 1988.
[21] A. L. Glebov, V. Panella, J. P. Toennies, F. Traeger, H. Weiss, S. Picaud, P. N. M. Hoang, and C. Girardet, Phys. Rev. B **61**, 14028 (2000).
[22] J. P. Toennies, F. Traeger, H. Weiss, S. Picaud, and P. N. M. Hoang, Phys. Rev. B **65**, 165427 (2002).
[23] H. K. Koski and E. Sandor, Acta Crystallogr., Sect. B: Struct. Crystallogr. Cryst. Chem. **31**, 350 (1975).
[24] R. K. McMullan, Å Kvick, and P. Popelier, Acta Crystallogr., Sect. B: Struct. Sci. **48**, 726 (1992).
[25] B. N. J. Persson and R. Ryberg, Phys. Rev. B **24**, 6954 (1981).
[26] *Helium Atom Scattering from Surfaces*, edited by E. Hulpke (Springer, Berlin, 1992).
[27] J. Vogt and H. Weiss, J. Chem. Phys. **119**, 1105 (2003).
[28] J. Vogt and H. Weiss, Surf. Sci. **491**, 155 (2001).
[29] J. Vogt, Ph.D. thesis, University of Hannover, 2001.
[30] J. Vogt and H. Weiss (unpublished).
[31] B. W. Holland and D. P. Woodruff, Surf. Sci. **36**, 488 (1973).
[32] G. Herzberg, *Molecular Spectra and Molecular Structure* (Van Nostrand, New York, 1945).
[33] J. D. Jackson, *Classical Electrodynamics* (Wiley, New York, 1962).
[34] R. I. Keir, D. W. Lamb, L. D. Ritchie, and J. N. Watson, Chem. Phys. Lett. **279**, 22 (1997).
[35] K. Kim and W. T. King, J. Mol. Struct. **57**, 201 (1979).
[36] P. Jona, M. Gussoni, and G. Zerbi, J. Phys. Chem. **85**, 2210 (1981).
[37] K. Shuler and C. E. Dykstra, J. Phys. Chem. A **104**, 11522 (2000).
[38] The KCl substrate was considered as a perfectly transparent material in the infrared with a constant refractive index of 1.47.
[39] According to Eq. (6) with the assumption $\sigma=3\sigma_{\mathrm{rand}}$ to account for the defined alignment of the molecules with respect to the external electric field.